

## Decay of Silicon Mounds: Scaling Laws and Description with Continuum Step Parameters

A. Ichimiya and K. Hayashi

*Department of Quantum Engineering, Nagoya University, Furo-cho, Chikusa-ku, Nagoya 464-8603 Japan*

E. D. Williams and T. L. Einstein

*Department of Physics, University of Maryland, College Park, Maryland 20742-4111*

M. Uwaha and K. Watanabe\*

*Department of Physics, Nagoya University, Furo-cho, Chikusa-ku, Nagoya 464-8602 Japan*

(Received 5 November 1999)

The decay of mounds about a dozen layers high on the Si(111)-(7 × 7) surface has been measured quantitatively by scanning tunneling microscopy and compared with analytic predictions for the power-law dependence on time predicted for a step-mediated decay mechanism. Conformably, we find an exponent 1/4 associated with the (3D) decay of the mound height and exponent 1/3 associated with the (2D) decay of top-layer islands. Using parameters from a continuum step model, we capture the essence of the kinetics. Qualitative features distinguish these mounds from multilayer islands found on metals.

PACS numbers: 68.35.Md, 61.16.Ch, 68.55.-a, 68.60.Dv

To advance understanding in surface science, it is crucial to be able to characterize systems in terms of a few macroscopic parameters rather than a myriad of microscopic energies in what amounts to a length-scale bridging approach. Success requires that parameters extracted from one sort of measurement can be exploited to study different properties. In particular, using the thermodynamic properties of steps [1] to predict the decay of nanostructures on surfaces has captured considerable interest lately. In a notable recent experiment, for example, Tanaka *et al.* [2] studied biperiodic  $\mu\text{m}$ -scale surface modulations on Si(100) and related their decay process to step crossing in surface mass transport. To obtain analytically tractable models, most theoretical work [3–6] has considered either (mono)periodic modulations or stacks of concentric circular islands, often called “wedding cakes.” Conical clusters might be viewed as representing structures with faceted sides, while paraboloids model rough surfaces. As capsulized in Table I, the evolution of such structures depends strongly on the shape of the cluster and on what limits the decay. In addition, scaling formulations make bold predictions regarding collapse of data with appropriately scaled axes [3]. Experimental work in this direction to date has treated structures with just a small number of layers [7,8]. In this report we make a direct experimental connection between the properties of a single-layer structure and a fully 3D nanoscale structure.

On silicon surfaces, decay rates for both single-layer, “two-dimensional (2D)” islands and 2D craters were previously measured at various temperatures with a scanning tunneling microscope (STM). The measured decay rate of the island radius varied as  $t^{1/2}$ , indicating (see Table I) that an attachment-detachment limited (ADL) process at step edges governs the decay of the 2D structures on this surface [9,10]. In this Letter we describe the decay of island mounds consisting of a stack of a dozen such layers on the

reconstructed Si(111) surface, allowing us to check and confirm both the proposed scaling expressions for the decay and the quantitative rate of the decay as predicted from the step-mediated mechanism.

The Si(111) specimens used in the present experiments are P doped,  $n$  type,  $3\ \Omega\ \text{cm}$  wafers of size  $1 \times 7 \times 0.3\ \text{mm}^3$ . Sample preparation and experimental procedure are the same as described earlier [9]. During imaging, the sample was heated by a direct current passing through the specimen in the range from 0.19 to 0.25 A, which corresponds to the range of temperatures from 440 to 485 °C. Temperatures of the specimen were measured by correlating the readings of a W-Re thermocouple to the heating current after the experiments. Silicon mounds were created by positioning an initially clean STM tip, with the tip current between 0 and 10 nA and the sample bias between  $-2$  and 2 V, at a chosen site for a few minutes [11]. The tip velocity during STM observation was  $3.8\ \mu\text{m/s}$ , which corresponds to a typical scanning time of about 10 s per frame. In scanning mode, the tip current and the sample bias were 0.2 nA and 1.5 V, respectively. The pressure during measurements was  $2 \times 10^{-8}\ \text{Pa}$ . We determined the number of atoms in each layer from the area of each bilayer in the STM images using the atomic density of the (111) bilayer, even though the terraces have the dimer-atom-stacking-fault (DAS) structure [12].

TABLE I. Exponent  $1/\alpha$  of time dependence  $t^{1/\alpha}$  of the radius of the top layer of an evolving cluster. Summary of dependence on the decay mechanism and on the cluster shape: cones [ $R(h) = A_1(h_0 - h)$ ], paraboloids [ $R(h) = A_2(h_0 - h)^{1/2}$ ], and monolayer islands [3,5,6].

Initial shape	Kinetics limited	Diffusion limited
Cone	1/4	1/4
Paraboloid	1/6	1/5
Single layer	1/2	1/3

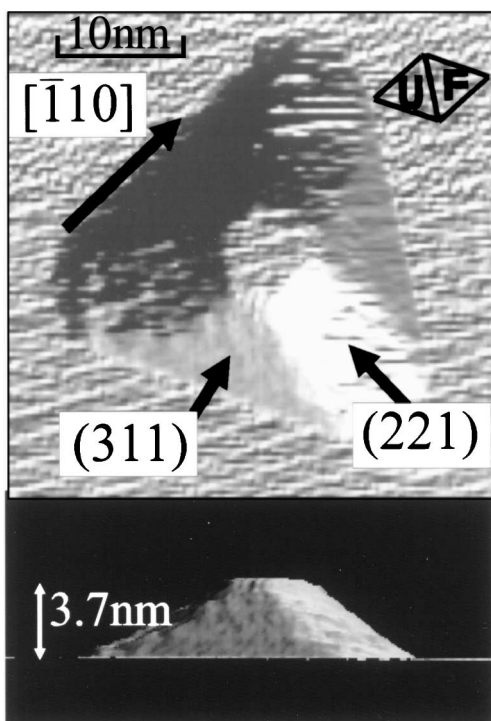


FIG. 1. Upper panel: Top view of a typical pyramidal 3D island created at 440 °C. This island is type *U*, i.e., unfaulted. The main facets are  $\{311\}$  and the intermediate facets are  $\{221\}$ . Lower panel: Side view of this truncated pyramid. The ratio  $A$  of the base radius to the height can be estimated as 1.6 given an initial extrapolated height of 15 layers and a base of 6824 atoms.

Figure 1 shows a typical mound produced by an STM tip on the Si(111)-(7 × 7) surface. Its edges are along the  $\langle 110 \rangle$  directions. Indices of the main facets are approximately  $\{311\}$ , and those of the small ones between them are  $\{221\}$ . The top of the mound is truncated by a (111) surface with the 5 × 5 DAS structure, which also characterizes the lower layers of the pyramid. The shape of the top terrace of the pyramid is nearly hexagonal, while the shape at the bottom is a rounded triangle. The long edges of the bottom layer lie along the unfaulted halves of the DAS structure of the substrate, as shown in Fig. 1. Twins of the mounds of Fig. 1 (rotated by 60° and oriented along the faulted halves of the DAS) are also produced with 25% probability. We call the former mound (which is produced with 75% probability) type *U*, and the latter kind of mound type *F*. At the interface between a type-*F* mound and the substrate, there is a stacking-fault layer, which is manifested by contrast in STM images of the DAS structure on the top terrace during the decay.

Figure 2 shows a typical set of the decay curves of a type-*U* mound, specifically for the structure depicted in Fig. 1. (A movie of this decay has been posted [13].) For each bilayer of the mound, there is a path of points showing the number of atoms in that layer as a function of time. In this particular case, the cluster was initially 12 bilayers high, the temperature was 440 °C, and scanning was done intermittently at 2 min time intervals. In other cases, the experiments were done at 465 and 485 °C, and

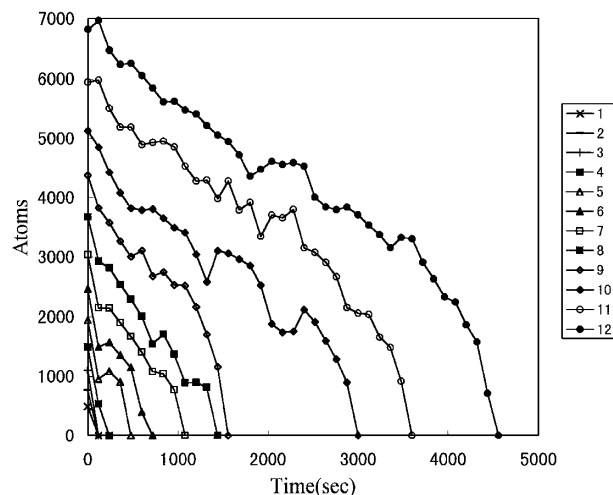


FIG. 2. Plot of the number of atoms in each layer of a cluster as a function of time during a typical decay of a *U* mound, along with the decay of the total number in the cluster.

scanning was done both intermittently [14] and continuously (viz., at 10 sec/frame) [15]. For each temperature and scan mode, about a half dozen runs were carried out. When a top layer finally disappears, emitting a relatively large number of atoms, the next layer should expand somewhat (cf. Ref. [8]) before resuming a monotonic decrease. This expectation is based on the assumption that an adatom attaches to the lower side of the bounding edge after descending the step. We do observe that a lower layer does expand at the extinction of a higher one. However, careful inspection of Fig. 2 shows that often it is not the new top layer that expands but rather the next layer below it. This observation suggests that the steps are partially permeable to mass crossing, though to a much smaller extent than in the decay of biperiodic gratings on Si(100) [2] (since step pairing is much weaker).

To quantify the decay in a format compatible with the step-continuum model predictions of Table I, we evaluate the vanishing time of each layer as a function of both the height of the mound and the initial radius of the layer. For a shape-preserving decay, the height of the mound will have a specific relationship to the layer radii as in Table I. Figure 3 shows an example of the plot of the height as a function of disappearance time in the form:

$$h_0 - h = Bt^{1/\alpha}, \quad (1)$$

appropriate for shape-preserving decay of a cone, where  $h_0$  is the extrapolated height of the initial structure, as done in the theoretical work of Israeli and Kandel [3]. For these experimental structures, the value of  $h_0$  is generally three or four bilayers greater than the height of the actual initial top layer, i.e., the height of the truncated cone.

The average values of  $\alpha$  and  $B$  evaluated for all observed *U*-type structures are listed in Table II. For both intermittent and continuous scanning, the value of  $\alpha$  is essentially  $4.0 \pm 0.1$  for the type-*U* mounds, indicating that the tip has a negligible effect on this value [14]. For type-*F*

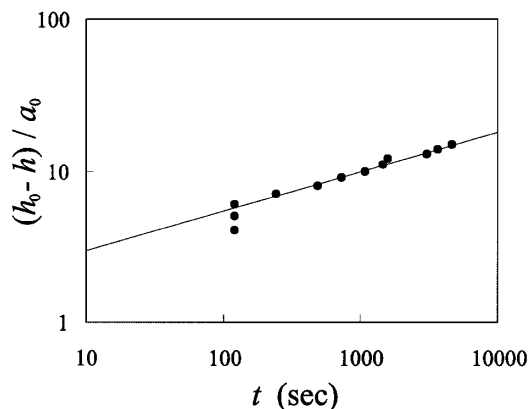


FIG. 3. Log-log plot of decrease in mound height (relative to extrapolated initial peak height) vs time, to check Eq. (1), for the mounds in Figs. 1 and 2. The first two disappearances of Fig. 2 at the shortest time (120 s) are not included, because the corresponding layers vanished before the second scan.

mounds, the exponent  $\alpha$  is smaller ( $\alpha = 3.0 \pm 0.2$ ), and the vanishing time of the bottom layer is about a third that of type  $U$ . The evident difference in both mechanism and rate, which we do not understand fully, may be due to a larger interface energy at the twin boundary at the base of the type- $F$  mound.

According to Table I for finite-size structures and to Israeli and Kandel's theory for infinite-size cones [3], the height of the cone decays with time according to a  $t^{1/4}$  power law. This theoretical result agrees very well with the present experimental result for type- $U$  mounds shown in Table II, despite the presence of some step bunching during the decay processes. Although a shape-preserving crystalline cone with zero step permeability is assumed in the theory, the power law agrees with the experimental result. The cone appears to be a good approximation for these isolated, single-pyramidal mounds of type  $U$ . This likely reflects stabilization of the  $\{311\}$  facets and implicitly adds the effects of step-step repulsion, an important determinant of surface morphology not explicitly included in our model.

The magnitude of the prefactor  $B$  in Table II can also be readily understood. In the earlier work on this surface [9], a monolayer island was found to decay at a rate of about 3 atoms/s at 440 °C [16]. This rate can be written as  $dN_{\text{isl}}/dt = 2\pi\Omega Kc_{\text{eq}}\tilde{\beta}/k_B T$ , the product of the atomic area ( $6.4 \text{ \AA}^2$ , viz.,  $\sim 12.8 \text{ \AA}^2$  per Si pair), the kinetic coefficient  $K$ , the equilibrium concentration of adatoms  $c_{\text{eq}}$ , and the reduced step stiffness  $\tilde{\beta}/k_B T$ . For shape-preserving decay of a cone,  $R = A_1(h_0 - h)$ , Uwaha and Watanabe

[6] have shown that the radius  $R_f$  of the top of the mound evolves, in the case of ADL dynamics, as

$$R_f^4(t) \approx 4a_0^2 A_1^2 \Omega^2 K c_{\text{eq}} (\tilde{\beta}/k_B T) t, \quad (2)$$

where  $a_0 \approx 3.1 \text{ \AA}$  is the interlayer spacing and  $A_1$  is the inverse slope of the cone as defined in the caption of Fig. 1. (Plots of the time dependence of  $R_f$  are consistent with  $R_f \propto t^{1/4}$ , particularly after removing points confounded by step bunching. Effects due to deviations of actual layers from the circular shape of the assumed cone may be compensated by the use of the experimental decay rate for single-layer islands that also have threefold symmetry.)

Combining these results, we estimate the prefactor  $B$  in Eq. (1) to be

$$B = [2a_0^2 \pi^{-1} A^{-2} \Omega (dN_{\text{isl}}/dt)]^{1/4}, \quad (3)$$

which yields  $2.6 \pm 0.3 \text{ \AA/s}^{1/4}$  at 440 °C. In Table II we compare these estimates with the values deduced above from fits of data such as in Fig. 3 by Eq. (1). Considering the simplicity of the model and the complexity of the real structures, the comparison is surprisingly good. From an Arrhenius plot of the measured values of  $B$ , we obtain  $B^4 = 10^{13 \pm 1} \exp(-1.6 \pm 0.1 \text{ eV}/k_B T) \text{ \AA}^4/\text{s}$ . This result also agrees well with the earlier analysis of 2D island decay [9], for which an activation barrier of 1.5 eV was obtained.

Villain made a related simple scaling prediction [4,5]: the time  $\tau$  necessary for a decaying circular island centered atop a second such island to vanish is proportional to the radius cubed for diffusion limited processes. For a conical structure (see Table I) this result also holds for an ADL process. Thus motivated, we investigated the possibility of a scaling law

$$\tau \propto N^\beta, \quad (4)$$

where  $N$  is the initial number of atoms in a top layer. In other words,  $N$  is determined, and the clock is started, at the instant that a top layer vanishes and the next layer below becomes the new top layer. Figure 4 gives a log-log plot of this top-layer extinction time vs essentially its initial area for many layers of seven different type- $U$  mounds at 440 °C. Although there is considerable scatter in the plot in Fig. 4, the exponent  $\beta$  is consistent with expectations. Specifically, we determine that  $\beta = 1.4 \pm 0.3$  [ $\approx 3/2$ ]. Similar behavior was found for the other  $U$  mounds as well as for the  $F$  mounds. We have calculated decay curves for both a single-layer, 2D island and a multilayer island using numerical solutions of the equations of motion, and evaluated the exponent  $\beta$  for each case. Simulations with ADL

TABLE II. Values of parameters for type- $U$  mounds.

Temperature	440 °C	465 °C	465 °C	485 °C
Time intervals	2 min	1 min	Continuous	30 s
$\alpha$ [Eq. (1)]	$4.0 \pm 0.1$	$3.9 \pm 0.05$	$3.9 \pm 0.1$	$4.0 \pm 0.2$
$B \text{ \AA/s}^{1/4}$ [Eq. (1)]	$4.8 \pm 0.9$	$6.1 \pm 0.4$	$6.2 \pm 0.4$	$6.7 \pm 0.5$
$dN_{\text{isl}}/dt$ (s $^{-1}$ ) [9]	3	6	24	11
Calc. $B$ [Eq. (3)]	$2.6 \pm 0.3$	$3.1 \pm 0.3$		$3.6 \pm 0.4$

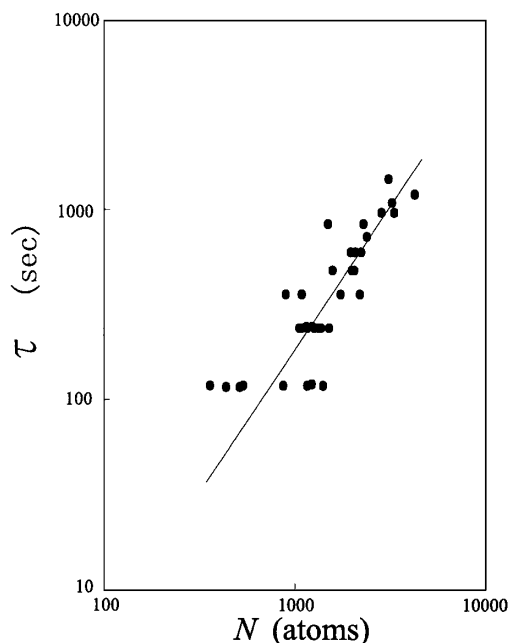


FIG. 4. Log-log plot of time vs atoms in the top layer of the cluster, to test the scaling prediction of Eq. (4).

processes [6] find an exponent  $\sim 1.0$  for the 2D island and  $\sim 1.4$  for the topmost layer of the mound. This theoretical result thus also agrees well with experiment for both 2D and 3D islands.

In addition to the above quantitative results, we have found several intriguing qualitative properties of the decay. In contrast to all the lower layers of a mound, which are concentric, the top layer tends to retract asymmetrically from the cone envelope so as to maintain contact with one side facet. There is, however, no evidence for avalanche behavior such as observed for several-layer-high clusters on Cu(111) [8]. We observe that when the mound is about four bilayers high, the triangular shape of the base evolves to a more nearly hexagonal shape via decay of the protrusions of the triangle. During the decay, the gradients of the facets change: The  $\{311\}$  facets evolve to approximately  $\{221\}$ , while the  $\{221\}$  facets tend to  $\{331\}$ .

There is evidence [17] that the  $\{311\}$  facet is more stable than the  $\{211\}$ ; then the observed evolution to  $\{211\}$  as the facet size becomes small suggests that the edge energy of the  $\{211\}$  and the (111) plane is less than the corresponding edge for the  $\{311\}$ . If so, then once the facets become small, the effect of the edge energy would become dominant, and the observed change in facet orientation would occur. The appearance of the hexagonal shape seems to correspond to this change of facet indices. When the mound decays to a single layer, it becomes a 2D island with truncated triangle shape which is rotated  $60^\circ$  from the bottom shape of the original type-*U* mound.

In summary, we have observed and modeled the decay of Si nanostructures containing fewer than 10 000 atoms. At this size scale, the structures display significant complexity at the atomic scale. In spite of the complexity, it

is possible to capture the essential physics to describe the kinetics using step thermodynamic parameters in a continuum step model. The effects of step-step repulsions and facet stabilization are contained implicitly in this model by the requirement that the conical shape is preserved during decay. The detailed effects of atomic-scale behavior at the step edges enter as the product of the step stiffness and the mobility, a value that was determined from observations of single-layer step structures.

The work of A. I. and K. H. was carried out under the support of a Grant-in-Aid for Creative Basic Research (No. 09NP1201) by the Ministry of Education, Science, Sports, and Culture (Monbusho). E. D. W. and T. L. E. were supported by NSF MRSEC Grant No. DMR-96-32521. M. U. was supported by "Research for the Future" of JSPS. The collaboration was sponsored by the Monbusho International Scientific Research Program: Joint Research (Grant No. 10044146). We acknowledge helpful conversations with D. Kandel, supported under U.S.-Israel BSF Grant No. 95-000268/3, and with H. P. Bonzel.

\*Present address: Hitachi ULSI Systems Co., 5-22-1 Josuihoncho Kodaira, Tokyo 187-8522, Japan.

- [1] H.-C. Jeong and E. D. Williams, *Surf. Sci. Rep.* **34**, 171 (1999).
- [2] S. Tanaka *et al.*, *Phys. Rev. Lett.* **78**, 3342 (1997).
- [3] N. Israeli and D. Kandel, *Phys. Rev. Lett.* **80**, 3300 (1998); *Phys. Rev. B* **60**, 5946 (1999).
- [4] J. Villain, *Europhys. Lett.* **2**, 531 (1986).
- [5] M. Uwaha, *J. Phys. Soc. Jpn.* **57**, 1681 (1988).
- [6] M. Uwaha and K. Watanabe, *J. Phys. Soc. Jpn.* **69**, 497 (2000).
- [7] K. Morgenstern *et al.*, *Phys. Rev. Lett.* **80**, 556 (1998).
- [8] M. Giesen, G. Schulze Icking-Konert, and H. Ibach, *Phys. Rev. Lett.* **80**, 552 (1998).
- [9] A. Ichimiya, Y. Tanaka, and K. Ishiyama, *Phys. Rev. Lett.* **76**, 4721 (1996).
- [10] A. Ichimiya, Y. Tanaka, and K. Hayashi, *Surf. Sci.* **386**, 182 (1998).
- [11] A. Ichimiya, Y. Tanaka, and K. Hayashi, *Surf. Rev. Lett.* **5**, 821 (1998).
- [12] K. Takayanagi *et al.*, *Surf. Sci.* **164**, 367 (1985).
- [13] <http://www.surf.nuqe.nagoya-u.ac.jp/intro/decay.html>
- [14] There is a limit to how large the interval between scans can be: For  $465^\circ\text{C}$  we tried a scanning interval of 1 min, only to find that  $\alpha \approx 3.7$ , indicating that the decay was too fast to be captured properly at this rate.
- [15] Specifically, continual scans were done only at  $465^\circ\text{C}$ . For the scans at  $465$  and  $485^\circ\text{C}$ , the time intervals in the intermittent mode was 1 min and 30 sec, respectively.
- [16] For intermittent scans, the decay rate can be obtained from the solid line in Fig. 5 of Ref. [9], namely,  $dN_{\text{isl}}/dt = 10^{11 \pm 1} \exp(-1.5 \pm 0.1 \text{ eV}/k_B T) \text{ s}^{-1}$ . The prefactor for hillock decay given in the text of Ref. [9] is too large by a factor of 2, as is that for crater decay. For continuous scanning, the corresponding rate (the solid line in Fig. 3 of Ref. [9]) is  $1.8 \times 10^{10} \exp(-1.3 \text{ eV}/k_B T) \text{ s}^{-1}$ .
- [17] A. A. Baski and L. J. Whitman, *Surf. Sci.* **392**, 69 (1997).